KSCE Journal of Civil Engineering (2018) 22(7):2256-2265

DOI 10.1007/s12205-017-0062-7

Geotechnical Engineering

pISSN 1226-7988, eISSN 1976-3808
www.springer.com/12205

Undrained Lateral Capacity of Rectangular Piles under a General Loading Direction and Full Flow Mechanism

Boonchai Ukritchon* and Suraparb Keawsawasvong**

Received January 14, 2017/Revised June 5, 2017/Accepted July 23, 2017/Published Online August 31, 2017

Abstract

New upper and lower bound solutions of undrained lateral capacity of rectangular piles under a general loading direction and full flow mechanism were investigated by using finite element limit analysis with plane strain condition. The true collapse loads of this problem were generally bracketed by computed upper and lower bound solutions to within 3%. Results were summarized in the form of three dimensionless variables, including soil–pile adhesion factor, pile aspect ratio, and lateral loading direction. Predicted failure mechanisms of laterally loaded rectangular piles associated with these parameters were examined and discussed. Approximate equations of failure envelopes for rectangular piles under a general loading direction were proposed for a convenient and accurate prediction of their undrained lateral capacity in practice.

Keywords: *laterally loaded pile, barrette, rectangular pile, lateral capacity, limit analysis, upper bound solution, lower bound solution*

1. Introduction

At present, there is an increase in demand for piles to carry more allowable load capacities in both vertical and lateral directions to support extremely large structures. This demand has driven new developments and improvements of cast–in–place pile construction technologies to achieve substantial pile capacities. Rectangular piles, known as barrettes, are cast–in–place reinforced concrete piles that have become more commonly used as deep foundations to support expressways, transmission towers, subway stations, and high–rise buildings (e.g., Ng *et al.*, 1999 and 2002; Ng and Lei, 2002; Thasnanipan and Taparaksa, 2002; Thasnanipan *et al.*, 2004; Lei and Ng, 2007; Taparaksa, 2015; Boonyatee *et al.*, 2015). When compared to a circular pile of comparable cross-sectional area, rectangular piles offer a number of advantages over circular piles, especially higher horizontal load and moment capacities.

In general, the ultimate lateral capacity of piles increases with depth from an initial low value at the ground surface to a maximum value at a certain depth, which remains constant at deeper pile lengths. This corresponds to a full flow failure mechanism around a pile (e.g., Murff and Hamilton, 1993), where the complete lateral translation of a pile at a depth relatively far from the ground surface essentially takes place under the plane strain condition. In the past, a large number of studies on the ultimate lateral capacity of piles in clay under the full flow failure mechanism have been investigated by various researchers, including slip line solutions of different pile sections (Broms, 1964), upper and lower bound solutions of single circular pile (Randolph and Houlsby, 1984; Martin and Randolph, 2006), and finite element limit analysis of two side–by–side circular piles with a symmetrical load (Georgiadis *et al.*, 2013a), a row of circular piles (Georgiadis *et al.*, 2013b) and two side–by–side circular piles with load inclination (Georgiadis *et al.*, 2013c). In addition, there have been significant numerical and experimental studies about lateral responses of monopiles in granular and cohesive materials under static and cyclic loadings, such as Lesny *et al*. (2007), Achumus *et al*. (2009), Hokmabadi *et al*. (2012), Lombardi *et al*. (2013), Bisoi and Haldar (2014), Depina *et al*. (2015), and Li *et al*. (2017). Recently, Keawsawasvong and Ukritchon (2016a) employed a finite element analysis to analyze the undrained lateral capacity of rectangular piles under the full flow failure mechanism, considering lateral loading along either their major or minor axes. However, their solutions were limited to only two loading directions. Up until now, there seems to be no solution available in the literature that considers the full flow failure capacity of rectangular piles under a general loading direction.

In this paper, new plasticity solutions of undrained lateral capacity of rectangular piles under a general loading direction and full flow failure mechanism were investigated by using the plane strain Finite Element Limit Analysis (FELA) software, OptumG2 (Krabbenhoft *et al.*, 2015). Approximate expressions of failure

*Associate Professor, Geotechnical Research Unit, Dept. of Civil Engineering, Faculty of Engineering, Chulalongkorn University, Bangkok 10330, Thailand (Corresponding Author, E-mail: boonchai.uk@gmail.com)

**Ph.D. Research Fellow, Geotechnical Research Unit, Dept. of Civil Engineering, Faculty of Engineering, Chulalongkorn University, Bangkok 10330, Thailand (E-mail: suraparb@hotmail.com)

envelopes of laterally loaded rectangular piles were also proposed based on a nonlinear regression of lower bound solutions. The results of this study are the most important aspects of stability evaluation of rectangular piles under a general loading. In addition, they can be employed to estimate the limiting resistance per unit length in the relationship between load and deflection along the pile length using the (p–y) curve method (e.g., Reese *et al.*, 2006).

2. Method of Analysis

Figure 1 shows the problem definition of the undrained lateral capacity of a rectangular pile under a general loading direction. It is assumed that below a certain depth from the ground surface, soil movements take place within this cross section, which corresponds to the full flow mechanism. Thus, the plane strain condition below that depth can be applied in the direction of pile depth. The rectangular pile has a width (B) and length (H) that correspond to the short and long dimensions of its cross section, where $B < H$. An inclined load (P) per unit length of the pile with respect to an angle β from y–axis is applied on its center to produce the full flow mechanism of rectangular pile under the undrained condition.

The clay has an isotropic and constant undrained shear strength (s_u) and obeys the rigid–perfectly plastic Tresca material with the associated flow rule. The shear strength at the soil-pile interface (s_{ui}) is controlled by its adhesion factor (α) as: $\alpha = s_{ui}/s_u$. Because of the assumption of the plane strain condition applied to the direction of pile depth, a weightless soil (i.e., $\gamma = 0$) is considered in the analysis. The ultimate lateral pile load can be expressed as the dimensionless load factor, N, which is a function of three dimensionless variables as:

$$N = \frac{2P}{s_u(B+H)} = f(\alpha, \frac{B}{H}, \beta) \tag{1a}$$

where B/H = Aspect ratio of rectangular pile

Three parametric studies of undrained lateral capacity of rectangular piles were performed to cover practical ranges of this problem, including B/H = 0.2 – 1.0, α = 0 (smooth) to 1 (rough), and β = 0° – 90° due to two symmetries through the vertical (y) and horizontal (x) axes of a rectangular pile.

It is well established that the interface parameters play significant role in the limit load of stability problems involving soil-structure interactions, such as bearing capacity of strip footings (Ukritchon *et al*., 2017; Ukritchon and Keawsawasvong, 2017), pullout capacity of suction caissons (Keawsawasvong and Ukritchon, 2016b; Ukritchon and Keawsawasvong, 2016), laterally loaded piles (Randolph and Houlsby, 1984; Martin and Randolph, 2006; Keawsawasvong and Ukritchon, 2016a; Keawsawasvong and Ukritchon, 2017c), stability of active trapdoors (Keawsawasvong and Ukritchon, 2017a), and limiting pressure behind soil gaps (Keawsawasvong and Ukritchon, 2017b). Recently, Fatahi *et al*. (2014) employed a three-dimensional finite element method to investigate an effect of interface parameters on a performance of laterally loaded piles. They reported that the interface strength reduction factor had a slight influence on predicted maximum pile bending moment, but had a notable effect on performance predictions of the pile-system subjected to the lateral loading.

In this study, interface elements are used around the perimeter of pile in order to reasonably simulate a soil-pile interaction. The model of interface parameter used in the previous studies of laterally loaded piles (Randolph and Houlsby, 1984; Martin and Randolph, 2006; Keawsawasvong and Ukritchon, 2016a; Keawsawasvong and Ukritchon, 2017c) is adopted and modelled as the cohesive type of interface that is controlled by the single parameter, commonly known as the adhesion factor (α), as shown below.

$$\alpha = s_{ui}/s_u \tag{1b}$$

where s_{ui} = Undrained shear strength at the interfaces (i.e., limiting shear stress)
s_u = Undrained shear strength of the surrounding soil

Thus, the shear tractions (τ_i) along the soil-pile interface must be smaller or equal to its interface undrained shear strength as:

$$|\tau_i| \le s_{ui} \tag{1c}$$

Note that Eq. (1c) is the special case of the cohesive-frictional type of interface governed by the Mohr-Coulomb failure criterion with zero friction angle. In practice, the concept of cohesive interface defined by the adhesion factor is generally employed in an estimation of a pile shaft capacity of a pile in cohesive soils (i.e., the "alpha" method, e.g., Fleming *et al*., 2008). In this study, the ratio of the adhesion factor is studied to produce the complete interface behavior of rectangular piles, ranging from perfectly smooth interface (α = 0) to perfectly rough interface (α = 1), where α = 0, 0.2, 0.4, 0.6, 0.8 and 1.0. In addition, the fully bonded soil-pile interface is also adopted, based on the previous modeling of interface parameters in laterally loaded piles (Randolph and Houlsby, 1984; Martin and Randolph, 2006; Keawsawasvong and Ukritchon, 2016a; Keawsawasvong and Ukritchon, 2017c) since the full-flow failure mechanism of soil around pile is sought, in which a separation between soil and pile is not permitted (i.e., full tension interface).

A plane strain numerical model of laterally loaded rectangular piles in OptumG2 is shown in Fig. 1. Note that the plane strain condition corresponds to the direction of the pile depth. The rectangular pile is defined as a rigid solid element that has a significant strength of Tresca criterion to ensure rigid behavior. A lateral load, P, inclined at an angle of β with respect to the vertical axis is treated by resolving into two components of uniform tractions in the vertical ($P\cos\beta/B$) and horizontal ($P\sin\beta/H$) directions, where each traction is applied at the top and right sides of the pile, respectively. These loadings cause the full flow failure mechanism around the rectangular pile, and are optimized in both upper and lower bound analyses. Due to two geometrical symmetries along the horizontal and vertical axes of the rectangular

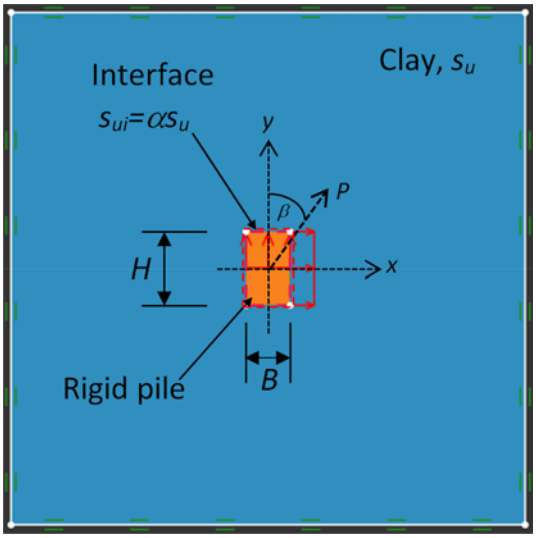

Fig. 1. Numerical Model of the Undrained Lateral Capacity of Rectangular Pile

pile, only the loading inclination from 0° to 90° is considered in the analyses.

The following summarizes the upper and lower bound formulations in OptumG2 that are related to analyses of ultimate lateral capacities of rectangular piles.

In the upper bound analysis, the soil mass is discretized into six–noded triangular elements. For each element, unknown velocity components of each node employ a quadratic interpolation within each element, and are continuous between adjacent elements. Velocity discontinuities are permitted at interface elements that are defined along the soil–pile perimeter. These velocity discontinuities are implemented by collapsing patches of regular triangular elements to zero thickness (Krabbenhoft *et al*., 2005; Lyamin *et al*., 2005). All external boundaries of the model are fixed only in the normal direction while the tangential direction is free. Constraints of kinematically admissible velocity conditions include velocity boundary conditions and compatibility and flow rule equations at triangular and interface elements. The objective function of upper bound calculation is defined to minimize the load (P) that is obtained through invoking the principle of virtual work by equating the rate of work done by external loads (i.e., the resolved vertical and horizontal uniform tractions) with the internal energy dissipation at triangular and interface elements. The upper bound optimization problem is cast as a Second–Order Cone Programming (SOCP) (e.g., Krabbenhoft *et al*., 2007; Makrodimopoulos and Martin, 2007), where the load P is minimized and subjected to the constraints of kinematic admissibility.

In the lower bound analysis, the soil mass is discretized into three–noded triangular elements. For each element, unknown stress components of each node employ a linear interpolation within the element. Unlike a conventional displacement–based finite element method, each element has its own unique node, resulting in possible stress discontinuities to happen along all shared edges of adjacent elements, including soil–pile interface elements. For all external boundaries of the lower bound model, zero shear traction is enforced along the tangential direction, while the normal traction is unconstrained in the normal direction. Constraints of statically admissible stress conditions include equilibrium equations at triangular elements and shared edges of stress discontinuities, stress boundary conditions, and no stress violation of yield criterion in the soil mass. The objective function of lower bound calculation is defined to maximize the load P, where the resolved vertical and horizontal uniform tractions acting on corresponding pile edges are treated as standard stress boundary conditions. The lower bound optimization problem is also cast as SOCP (e.g., Krabbenhoft *et al.*, 2007; Makrodimopoulos and Martin, 2006), where the load P is maximized and subjected to the constraints of static admissibility.

For both upper and lower bound calculations, the size of the model is chosen to be large enough that the plastic zone is contained within the domain, and does not intersect all boundaries. Thus, the computed limit load is not altered by increasing the domain size nor affected by the boundaries. The upper and lower bound solutions are solved by using the general purpose optimization solver SONIC with SOCP algorithm (Krabbenhoft *et al.*, 2015).

An automatically adaptive mesh refinement, a powerful feature in OptumG2, was employed in both the upper and lower bound analyses to determine the tight upper and lower bound solutions. Five adaptive steps with an increase of the initial mesh of 5,000 elements to a final mesh of 10,000 elements were used for all analyses in which this setting was quantitatively enough to obtain an accurate solution. Full details of numerical FELA formulation in OptumG2 and extensive reviews of FELA can be found in Krabbenhoft *et al.* (2015) and Sloan (2013), respectively.

It should be noted that according to the plastic bound theorems (Drucker *et al*., 1952), the plastic limit load of a problem is not affected by initial stresses or deformations provided that the problem geometry is essentially unaltered (see Chen, 1975). Consequently, initial stresses or deformations are not considered in the LB and UB analyses, respectively. Note that the effects of initial stresses or deformations have never been considered in tremendous applications of limit analysis to stability problems in geomechanics (see Chen, 1975).

3. Results and Comparisons

Figures 2-3 shows an influence of the lateral loading direction on incremental displacement vectors of rectangular piles, where $\alpha = 1$ and $B/H = 1$, 0.2. As the loading direction is changed, the plastic flow and size of plastic yielding zone are skewed towards the direction of lateral load. Similar failure modes can be observed for the pile aspect ratio of 0.2. The comparisons of predicted failure mechanisms of rectangular piles that are affected by B/H and α are shown in Fig. 4, where $B/H = 0.2$, 0.6 and 1.0 and $\beta = 45°$. The shape of the flow–around mechanism and corresponding size of the plastic zone of rectangular piles are predominantly controlled by the adhesion factor. For square piles, the rough case corresponds to a lemniscatic shear band

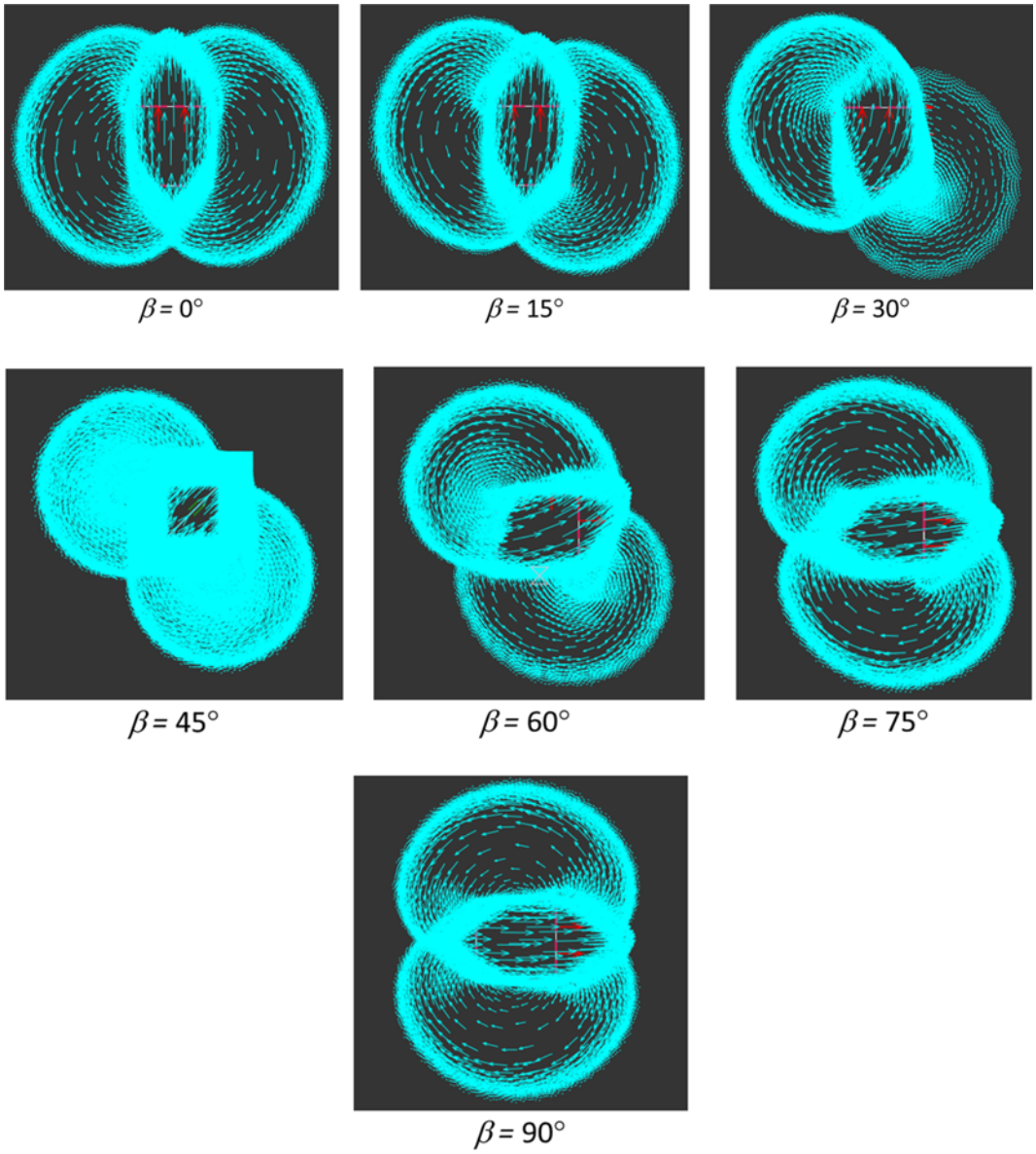

Fig. 2. Comparison of the Incremental Displacement Vectors for Rectangular Piles with *B/H* = 1 and α = 1

illustrated by two zones of circular arc shear bands that join along the diagonal line of the rectangular pile while the smooth case corresponds to a capsule shaped type of shear band. A decrease of pile aspect ratio results in a skewed failure mechanism of lemeniscate or capsule shape.

The influences of *B/H*, α and β on *N* are illustrated in Fig. 5. For all parametric studies, the exact *N* factor can be accurately bracketed by the computed bound solutions, where the differences between UB and LB solutions are small within 3% of the average solutions. Such small differences indicate the accurate predictions in the *N* factor since the adaptive mesh refinement in OptumG2 was utilized in both UB and LB simulations for all cases.

A complicated nonlinear relationship between *N* and *B/H* was found. For $\beta = 0° - 30°$, an increase of pile aspect ratio results in an increase of the lateral capacity of the rectangular pile. On the other hand, for $\beta = 45° - 90°$, there are four different patterns of *N*: i) monotonically asymptotic function (e.g., $\beta = 45°$, Fig. 5(d)), ii) concave function (e.g., $\beta = 60°$, Fig. 5(e)), iii) mixed decreasing and concave function (e.g., $\beta = 75°$, Fig. 5(f)), and iv) monotonically decreasing function (e.g., $\beta = 90°$, Fig. 5(g)).

Figures 5(a) and 5(g) also illustrate the comparisons in the *N* factor of rectangular piles loaded along either their vertical ($\beta = 0°$) or horizontal ($\beta = 90°$) axes between computed bound solutions and existing solutions by finite element analysis (Keawsawasvong and Ukritchon, 2016a), respectively. Generally, the predicted values and trends in the lateral capacity as a function of the pile aspect ratio agree very well with that of the existing solutions for all adhesion factors. Particularly, the present study has made a significant improvement over the previous finite element solutions

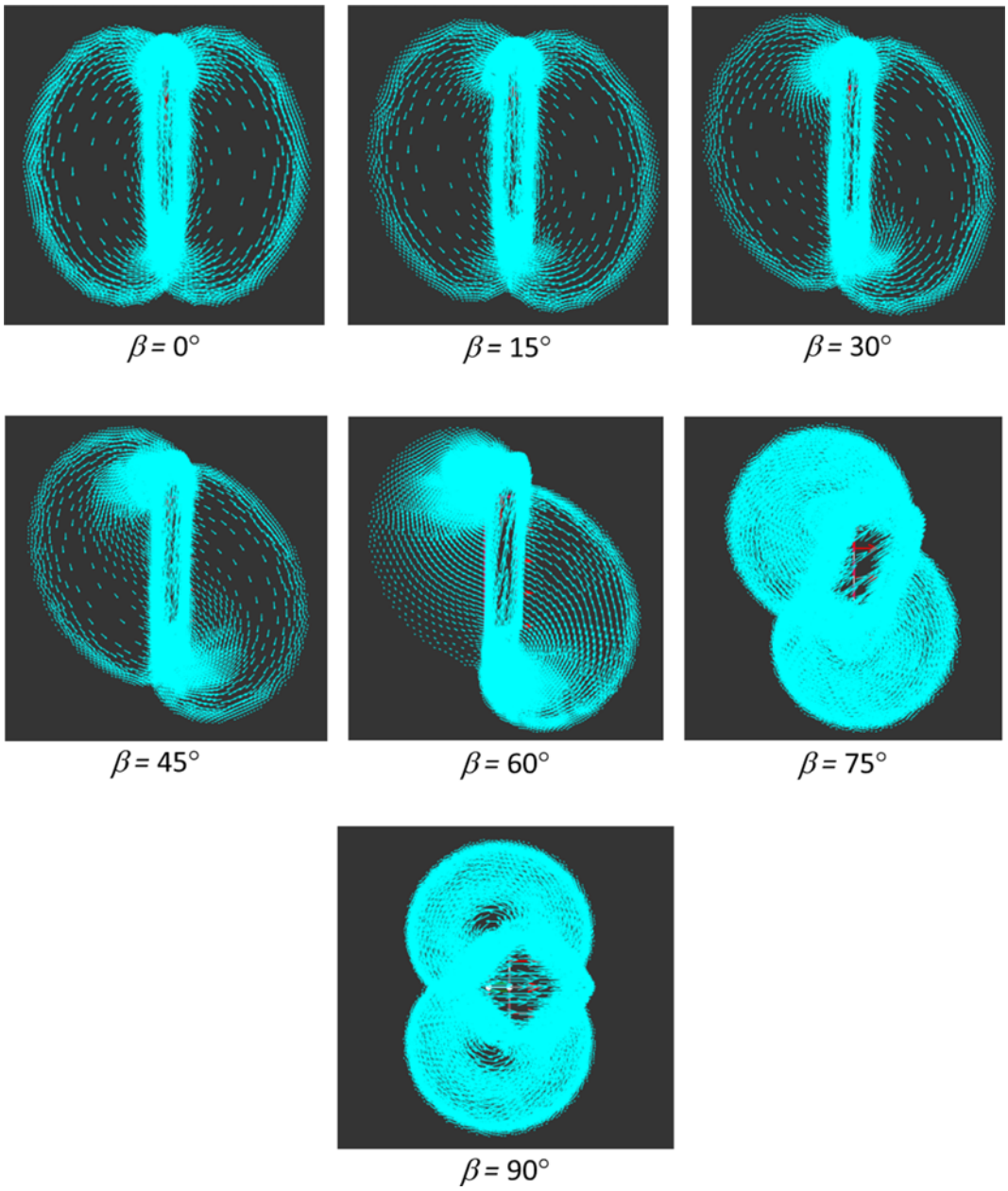

Fig. 3. Comparison of the Incremental Displacement Vectors for Rectangular Piles with B/H = 0.2 and α = 1

of rectangular piles in those two directions by about 1 – 6%.

4. Approximate Expression

As described earlier, the relationships between the dimensionless load factor (N) and loading inclination (β) are very complicated (see Figs. 5(a)-5(g)), which involves with different curve characteristics, such as monotonic increase, decrease, or asymptote, etc. Thus, it is not convenient to develop an approximate single equation that possesses such characteristics. The effect of combined loading on rectangular piles can be represented by using another normalization in which the total inclined load factor (N) is resolved into two components along the y and x axes, namely the vertical load factor (i.e., $F_y = N\cos\beta$) and the horizontal load factor ($F_x = N\sin\beta$). Then, the F_y and F_x factors are divided by the purely vertical capacity (F_{y0} at $\beta = 0°$) and the purely horizontal capacity (F_{x0} at $\beta = 90°$), respectively. A new normalized two-dimensional plot between $f_x = F_x/F_{x0}$ and $f_y = F_y/F_{y0}$ is developed, which represents the failure envelope for the combined loading of rectangular piles, as shown in all symbols in Fig. 6. Each subplot of the figure corresponds to a constant aspect ratio of rectangular pile (B/H), while each contour line in the subplot corresponds to a constant of adhesion factor (α). In general, the failure envelope looks like a locus of circle that becomes slightly distorted with a decrease of B/H and expands in size with an increase of α.

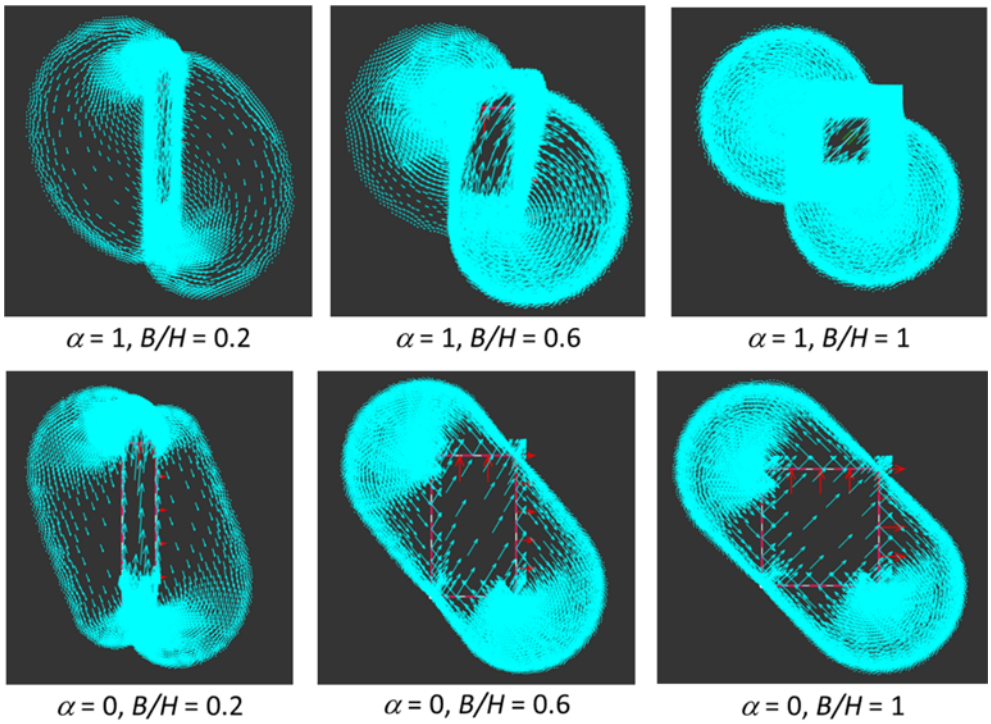

Fig. 4. Comparison of the Incremental Displacement Vectors for Rectangular Piles with $\beta = 45°$, and $\alpha = 1$ and 0

By employing a nonlinear regression analysis to the lower bound solutions, an approximate single expression developed from a modified circular locus is proposed to describe the failure envelope of rectangular piles under a general loading direction as follows:

$$f_x = \left[1 - {f_y}^m\right]^{(1/n)} \tag{2}$$

$$f_y = \frac{F_y}{F_{y0}} \tag{3}$$

$$f_x = \frac{F_x}{F_{x0}} \tag{4}$$

$$F_{y0} = \frac{4\alpha + (a_3\alpha^2 + a_2\alpha + a_1)(B/H)}{1 + (\alpha a_5 + a_4)(B/H)} \tag{5}$$

$$F_{x0} = \frac{4 + 6\pi + \left(a_3\alpha^2 + (4 + a_2)\alpha + a_1 - (4 + 6\pi)\right)(B/H)}{1 + (\alpha a_5 + a_4)(B/H)} \tag{6}$$

$$n = a_6 + \alpha a_7 + a_8\alpha\left(1 - \frac{B}{H}\right) \tag{7}$$

$$m = a_6 + \alpha a_7 + a_9\alpha\left(1 - \frac{B}{H}\right) \tag{8}$$

where

$$F_y = \frac{2P\cos\beta}{s_u(H + B)} = N\cos\beta$$

$$F_x = \frac{2P\sin\beta}{s_u(H + B)} = N\sin\beta$$

$a_1 - a_9$ are constant coefficients

The terms F_y and F_x represent the dimensionless load factors that are resolved into the vertical and horizontal directions, respectively. Two factors F_{y0} and F_{x0} correspond to the lateral capacities of a rectangular pile that are purely loaded in vertical ($\beta = 0°$) and horizontal ($\beta = 90°$) directions, respectively. For the special case of plate (i.e., $B/H = 0$) loaded either along the vertical or horizontal directions, these factors are: $F_{y0} = 4\alpha$ and $F_{x0} = 4 + 6\pi$. Note that the former can be obtained from the vertical static equilibrium by integrating the fully mobilized shear traction along both sides of the plate length while the latter is Rowe (1978)'s upper bound solution of the ultimate lateral capacity of deeply embedded plate anchors in the full flow failure mechanism, which is independent of α. For a square pile, the condition of $F_{y0} = F_{x0}$ is perfectly achieved using both Eqs. (5) and (6).

According to Eq. (2), the failure envelope of rectangular piles in the plot of f_y versus f_x produces one quarter circular–like locus that ranges from zero to unity for both axes. In a general case of a rectangular pile (i.e., $B/H \neq 1$), the proposed envelope is not symmetrical on the equality line, $f_y = f_x$. However, when the pile becomes square (i.e., $B/H = 1$), the power terms for f_y and f_x become identical (i.e., $m = n$), and hence the failure envelope is symmetrical on that line. This is because the solutions of a square pile have the symmetry at $\beta = 45°$.

Since a safe estimate on the true limit load can be obtained from a lower bound solution, computed lower bound solutions of rectangular piles were employed to determine the optimal solution of constant coefficients ($a_1 - a_9$) by a nonlinear regression analysis, as summarized in Table 1. Comparison of failure envelopes among different adhesion factors is illustrated in Fig. 6. For each case, the predicted failure envelope corresponds very well with

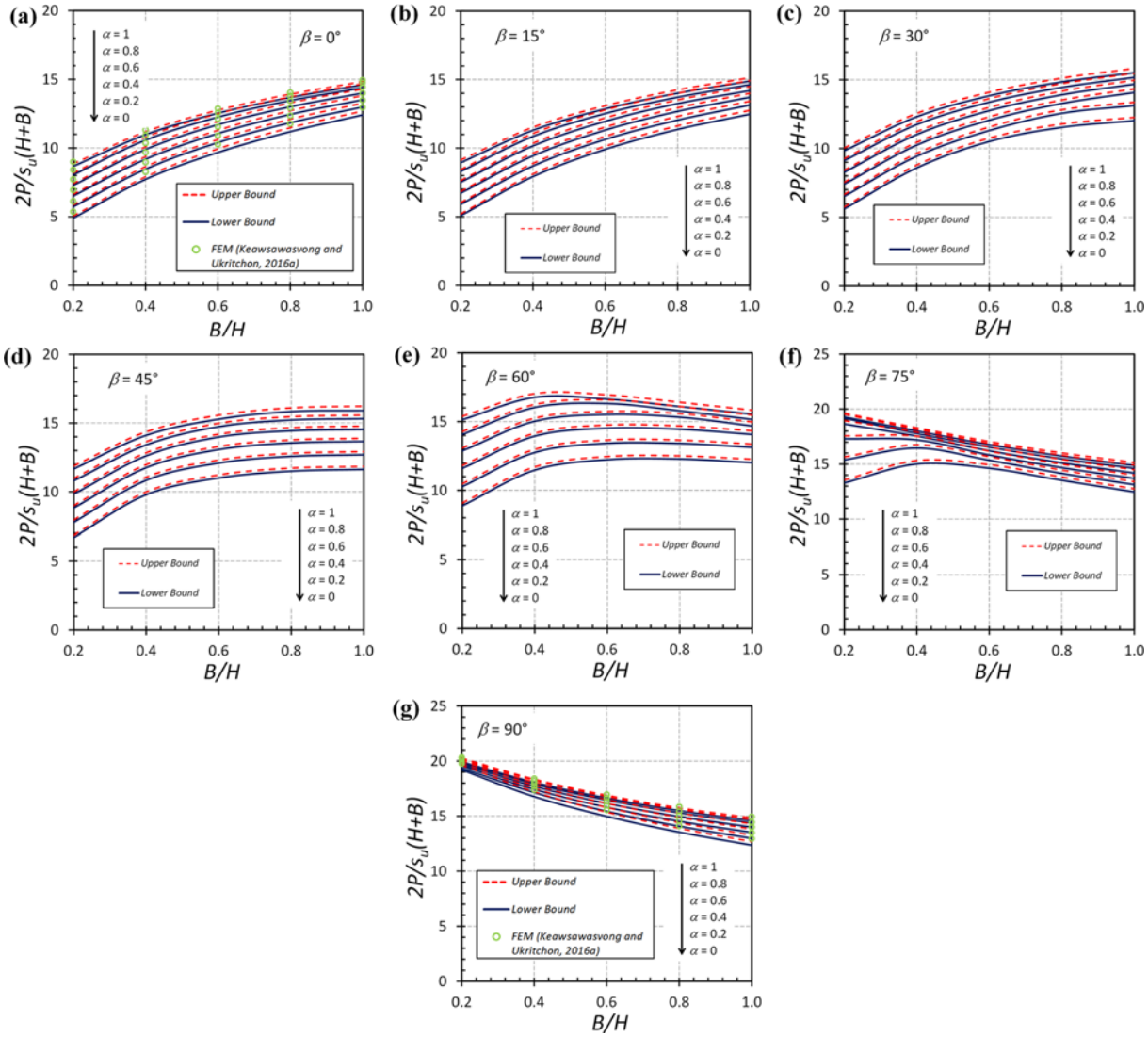

Fig. 5. Relationship between the Dimensionless Load Factor (*N*) and Pile Aspect Ratio (*B/H*) for: (a) $\beta = 0°$, (b) $\beta = 15°$, (c) $\beta = 30°$, (d) $\beta = 45°$, (e) $\beta = 60°$, (f) $\beta = 75°$, (g) $\beta = 90°$

Table 1. Optimal Value of Statistical Constants for the Proposed Failure Envelope

a_1	a_2	a_3	a_4	a_5	a_6	a_7	a_8	a_9
29.0652	8.0290	–2.1632	1.3163	0.2987	1.9010	0.6606	–0.9022	2.1240

computed lower bound solutions. These comparisons confirm the dependency of the failure envelope of rectangular piles upon the adhesion factor at the soil–pile interface and the pile aspect ratio. In general, as α increases, the failure envelope becomes slightly distorted and expands in size. Note that the failure envelope of square piles is symmetrical at the equality line, $f_y = f_x$.

5. Remarks

In this study, a simplified approach of a full flow failure mechanism around a pile was employed, and undrained behavior of clays with a perfectly plastic material and associated flow rule was assumed. Thus, the results are restricted to an application of a short-term loading rather than a long-term loading while a pre-failure deformation behavior of clay is neglected. For the long term loading, this effect causes a consolidation of the clay, thereby resulting in an increase of undrained shear strength with time. A solution of an initial excess pore water pressure generated immediately after an applied lateral load and before the start of consolidation can be obtained from the elastic solution by Baguelin *et al*. (1977) using incompressible conditions, since this prediction was shown to be in excellent agreement with the FE results (Osman and Randolph, 2012). Then, a consolidation solution of clays around a laterally loaded pile can be determined

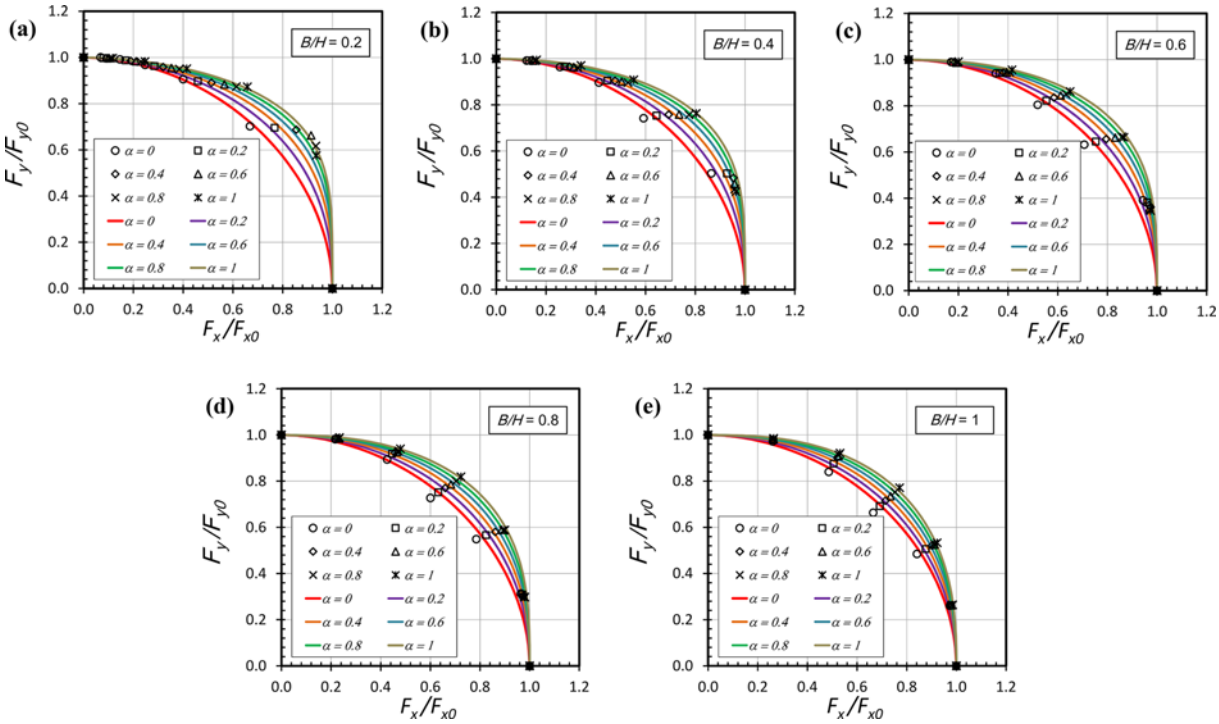

Fig. 6. Comparison of the Failure Envelope between the Proposed Equation and Lower Bound Solution for: (a) *B/H* = 0.2, (b) *B/H* = 0.4, (c) *B/H* = 0.6, (d) *B/H* = 0.8, (e) *B/H* = 1.0

by an analytical method (e.g., Osman and Randolph, 2010; Osman and Randolph, 2012) or by a finite element approximation (e.g., Carter and Booker, 1981). Since available consolidation solutions were limited to circular shape of pile, particular care should be taken to approximate a solution of a rectangular pile from that of a circular pile. Finally, a resulting increase of undrained shear strength of clay due to the consolidation can be practically estimated from the SHANSEP equation (Ladd, 1991), an empirical power law relationship based on its stress history.

The presented results of a laterally loaded rectangular pile can be applied for a stability evaluation of a pile under lateral loading during earthquakes. For a simplified approximation of this problem, the method of pseudo-static analysis commonly used in slope stability (e.g., Koppula, 1984; Baker *et al*., 2006) may be adopted in which two horizontal (*x, y*) earthquake ground motion records are utilized. The earthquake inertial forces of pile are calculated from two horizontal seismic coefficients in *x* and *y* directions, and assumed to be the applied lateral load in each direction. For a more accurate seismic analysis, the seismic lateral load acting on pile can be obtained by employing the three-dimensional (3D) numerical simulations with three directions of earthquake ground motion records, as proposed by Hokmabadi and Fatahi (2016). They suggested that 3D finite element method or 3D finite difference method that takes into account of a complete analysis of soil-structure interaction should be performed, including the full modeling of superstructures of building frames (i.e., column, beam, floor slab), pile cap, piles, soils, and soil-pile interface. In addition, nonlinear material models with hysteretic damping as well as geometric nonlinearities (uplifting, gapping and *P*-Δ effects) should also be considered in 3D numerical simulations. Interested readers are referred the work by Hokmabadi and Fatahi (2016) for a detailed description of the accurate seismic modeling. Once the seismic lateral load acting on pile is obtained by means of the pseudo-static analysis or 3D seismic numerical simulations, the safety analysis of laterally loaded pile during earthquakes can be conveniently performed using either the proposed failure envelopes in Fig. 6 or the approximate expression in Eq. (2).

6. Conclusions

New plasticity solutions of undrained lateral capacity of rectangular piles under a general loading direction and full flow mechanism were examined by finite element limit analysis. Approximate expressions were proposed in terms of the failure envelope that was a function of its lateral capacity with respect to purely vertical and horizontal directions. These capacities and the curvature of failure envelope were controlled by adhesion factor and pile aspect ratio, resulting in one quarter distorted circular–like envelope. The proposed expressions serve as a convenient and accurate tool for a prediction of undrained lateral capacity of rectangular piles under a general loading direction in practice.

References

Achmus, M., Kuo, Y. S., and Abdel-Rahman, K. (2009). "Behavior of monopile foundations under cyclic lateral load." *Computers and*

Geotechnics, Vol. 36, No. 5, pp. 725-735, DOI: 10.1016/j.compgeo.2008.12.003.

Baguelin, F., Frank, R., and Said, Y. H. (1977). "Theoretical study of lateral reaction mechanism of piles." *Geotechnique*, Vol. 27, No. 3, pp. 405-434, DOI: 10.1680/geot.1977.27.3.405.

Baker, R., Shukha, R., Operstein, V., and Frydman, S. (2006). "Stability charts for pseudo-static slope stability analysis." *Soil Dynamics and Earthquake Engineering*, Vol. 26, No. 9, pp. 813-823, DOI: 10.1016/j.soildyn.2006.01.023.

Bisoi, S. and Haldar, S. (2014). "Dynamic analysis of offshore wind turbine in clay considering soil–monopile–tower interaction." *Soil Dynamics and Earthquake Engineering*, Vol. 63, pp. 19-35, DOI: 10.1016/j.soildyn.2014.03.006.

Boonyatee, T., Tongjarukae, J., Uaworakunchai, T., and Ukritchon, B. (2015). "A review on design of pile foundations in Bangkok." *Geotechnical Engineering Journal of the SEAGS & AGSSEA*, Vol. 46, No. 1, pp. 76-85.

Broms, B. B. (1964). "Lateral resistance of piles in cohesive soils." *Journal of the Soil Mechanics & Foundation*, Vol. 90, No. 2, pp. 27-63.

Carter, J. P., and Booker, J. R. (1981). "Consolidation due to lateral loading of a pile." *Proc., 10th Int. Conf. on Soil Mechanics and Foundation Engineering*, Balkema, Rotterdam, Netherlands, pp. 647-650.

Chen, W. F. (1975). *Limit analysis and soil plasticity*. Elsevier, Amsterdam, The Netherlands.

Depina, I., Le, T. M. H., Eiksund, G., and Benz, T. (2015). "Behavior of cyclically loaded monopile foundations for offshore wind turbines in heterogeneous sands." *Computers and Geotechnics*, Vol. 65, pp. 266-277, DOI: 10.1016/j.compgeo.2014.12.015.

Drucker, D. C., Prager, W., and Greenberg, H. J. (1952). "Extended limit design theorems for continuous media." *Quarterly of Applied Mathematics*, Vol. 9, No. 4, pp. 381-389.

Fatahi, B., Basack, S., Ryan, P., Zhou, W. H., and Khabbaz, H. (2014). "Performance of laterally loaded piles considering soil and interface parameters." *Geomechanics and Engineering,* Vol. 7, No. 5, pp. 495-524, DOI: 10.12989/gae.2014.7.5.495.

Fleming, K., Weltman, A., Randolph, M., and Elson, K. (2008). *Piling engineering (3rd Edition)*, Taylor & Francis, New York, NY, USA.

Georgiadis, K., Sloan, S. W., and Lyamin, A. V. (2013a). "Ultimate lateral pressure of two side–by–side piles in clay." *Géotechnique*, Vol. 63, No. 9, pp. 733-745, DOI: 10.1680/geot.12.P.030.

Georgiadis, K., Sloan, S. W., and Lyamin, A. V. (2013b). "Undrained limiting lateral soil pressure on a row of piles." *Computers and Geotechnics*, Vol. 54, pp. 175-184, DOI: 10.1016/j.compgeo.2013.07.003.

Georgiadis, K., Sloan, S. W., and Lyamin, A. V. (2013c). "Effect of loading direction on the ultimate lateral soil pressure of two piles in clay." *Géotechnique*, Vol. 63, No. 13, pp. 1170-1175, DOI: 10.1680/geot.13.T.003.

Hokmabadi, A. S. and Fatahi, B. (2016). "Influence of foundation type on seismic performance of buildings considering soil–structure interaction." *International Journal of Structural Stability and Dynamics*, Vol. 16, No. 8, pp.1550043, DOI: 10.1142/S0219455415500431.

Hokmabadi, A. S., Fakher, A., and Fatahi, B. (2012). "Full scale lateral behaviour of monopiles in granular marine soils." *Marine Structures*, Vol. 29, No. 1, pp.198-210, DOI: 10.1016/j.marstruc.2012.06.001.

Keawsawasvong, S. and Ukritchon, B. (2016a). "Ultimate lateral capacity of two dimensional plane strain rectangular pile in clay." *Geomechanics & Engineering*, Vol. 11, No. 2, pp. 235-252, DOI: 10.12989/gae.2016.11.2.235.

Keawsawasvong, S. and Ukritchon, B. (2016b). "Finite element limit analysis of pullout capacity of planar caissons in clay." *Computers and Geotechnics*, Vol. 75, pp. 12-17, DOI: 10.1016/j.compgeo.2016.01.015.

Keawsawasvong, S. and Ukritchon, B. (2017a). "Undrained stability of an active planar trapdoor in non-homogeneous clays with a linear increase of strength with depth." *Computers and Geotechnics*, Vol. 81, pp. 284-293, DOI: 10.1016/j.compgeo.2016.08.027.

Keawsawasvong, S. and Ukritchon, B. (2017b). "Undrained limiting pressure behind soil gaps in contiguous pile walls." *Computers and Geotechnics*, Vol. 83, pp. 152-158, DOI: 10.1016/j.compgeo.2016.11.007.

Keawsawasvong, S. and Ukritchon, B. (2017c). "Undrained lateral capacity of I-shaped concrete piles." *Songklanakarin Journal of Science and Technology*. (In press)

Koppula, S. D. (1984). "Pseudo-static analysis of clay slopes subjected to earthquakes." *Geotechnique*, Vol. 34, No. 1, pp.71-79, DOI: 10.1680/geot.1984.34.1.71.

Krabbenhoft, K., Lyamin, A. V., and Sloan, S. W. (2007). "Formulation and solution of some plasticity problems as conic programs." *International Journal of Solids and Structures*, Vol. 44, pp. 1533-1549, DOI: 10.1016/j.ijsolstr.2006.06.036.

Krabbenhoft, K., Lyamin, A. V., Hjiaj, M., and Sloan, S. W. (2005). "A new discontinuous upper bound limit analysis formulation." *International Journal for Numerical Methods in Engineering*, Vol. 63, pp. 1069– 1088, DOI: 10.1002/nme.1314.

Krabbenhoft, K., Lyamin, A., and Krabbenhoft, J. (2015). *Optum computational engineering (OptumG2)*, Available on, www.optumce.com

Ladd, C. C. (1991). "Stability evaluations during stage construction." *Journal of Geotechnical Engineering*, Vol. 117, No. 4, pp. 540-615.

Lei, G. H. and Ng, C. W. W. (2007). "Rectangular barrettes & circular bored piles in saprolites." *Proc., the Institution of Civil Engineers*, Geotechnical Engineering, Vol. 160, No. 4, pp. 237-242, DOI: 10.1680/geng.2007.160.4.237.

Lesny, K., Paikowsky, S. G., and Gurbuz, A. (2007). "Scale effects in lateral load response of large diameter monopiles." *Geo-Denver 2007: new peaks in geotechnics*, Colorado: ASCE.

Li, W., Zhu, B., and Yang, M. (2017). "Static response of monopile to lateral load in overconsolidated dense sand." *Journal of Geotechnical and Geoenvironmental Engineering*, Vol. 143, No. 7, pp. 04017026, DOI: 10.1061/(ASCE)GT.1943-5606.0001698.

Lombardi, D., Bhattacharya, S., and Wood, D. M. (2013). "Dynamic soil–structure interaction of monopile supported wind turbines in cohesive soil." *Soil Dynamics and Earthquake Engineering*, Vol. 49, pp. 165-180, DOI: 10.1016/j.soildyn.2013.01.015.

Lyamin, A. V., Krabbenhoft, K., Abbo, A. J., and Sloan, S. W. (2005). "General approach to modelling discontinuities in limit analysis." P*roceedings of IACMAG*, Turin, Italy.

Makrodimopoulos, A. and Martin, C. M. (2006). "Lower bound limit analysis of cohesive–frictional materials using second–order cone programming." *International Journal for Numerical Methods in Engineering*, Vol. 66, pp. 604-634, DOI: 10.1002/nme.1567.

Makrodimopoulos, A. and Martin, C. M. (2007). "Upper bound limit analysis using simplex strain elements and second–order cone programming." *International Journal for Numerical and Analytical Methods in Geomechanics*, Vol. 31, pp. 835-865, DOI: 10.1002/nag.567.

Martin, C. M. and Randolph, M. F. (2006). "Upper–bound analysis of lateral pile capacity in cohesive soil." *Géotechnique*, Vol. 56, No. 2,

pp. 141-145.

Muff, J. D., and Hamilton, J. M. (1993). "P–Ultimate for undrained analysis of laterally loaded piles." *Journal of Geotechnical Engineering*, Vol. 119, No. 1, pp. 91-107.

Ng, C. W. W. and Lei, G. H. L. (2002). "Performance of long rectangular barrettes in Granitic saprolites." *J. Geotech. Geoenviron. Eng.*, Vol. 129, No. 8, pp. 685-696, DOI: 10.1061/(ASCE)1090-0241(2003)129%3A8(685).

Ng, C. W. W., Rigby, D. B., Lei, G. H., and Ng, S. W. L. (1999). "Observed performance of a short diaphragm wall panel." *Géotechnique*, Vol. 49, No. 5, pp. 681-694, DOI: 10.1680/geot.1999.49.5.681.

Ng, C. W. W., Rigby, D.B., Ng, S. W., and Lei, G. H. L. (2002). "Field studies of well–instrumented barrette in Hong Kong." *J. Geotech. Geoenviron. Eng*., Vol. 126, No. 1, pp. 60-73, DOI: 10.1061/(ASCE)1090-0241(2001)127:5(466).

Osman, A. S. and Randolph, M. F. (2010). "Response of a solid infinite cylinder embedded in a poroelastic medium and subjected to a lateral load." *International Journal of Solids and Structures*, Vol. 47, Nos. 18-19, pp. 2414-2424, DOI: 10.1016/j.ijsolstr.2010.05.001.

Osman, A. S. and Randolph, M. F. (2012). "Analytical solution for the consolidation around a laterally loaded pile." *International Journal of Geomechanics*, Vol. 12, No. 3, pp. 199-208, DOI: 10.1061/%28ASCE%29GM.1943-5622.0000123.

Randolph, M. F. and Houlsby, G. T. (1984). "The limiting pressure on circular pile loaded laterally in cohesive soil." *Géotechnique*, Vol. 34, No. 4, pp. 613-623, DOI: 10.1680/geot.1984.34.4.613.

Reese, L., Isenhower, W., and Wang, S.T. (2006). *Analysis & design of shallow & deep foundations*. Hoboken, John Wiley & Sons, Inc.

Rowe, R. K. (1978). *Soil structure interaction analysis & its application to the prediction of anchor behavior*, Thesis, University or Sydney.

Sloan, S. W. (2013). "Geotechnical stability analysis." *Géotechnique*, Vol. 63, No. 7, pp. 531-572, DOI: 10.1680/geot.12.RL.001.

Teparaksa, W. (2015). "Deep barrette pile capacity with aging effect." *Geotechnical Engineering Journal of the SEAGS & AGSSEA*, Vol. 46, No. 2, pp. 68-76.

Thasnanipan, N., Aye, Z. Z., and Teparaksa, W. (2002). "Barrette of over 50,000 kN ultimate capacity constructed in the multi–layered soil of Bangkok." *Geotechnical Special Publication*, 116II, pp. 1073-1087, DOI: 10.1061/40601(256)76.

Thasnanipan, N., Aye, Z. Z., Singtogaw, K., and Pravesvararat, S. (2004). "Current practice & future trends of cast–in–place deep foundation in Thailand." *Geotechnical Special Publication*, Vol. 125, pp. 128-139, DOI: 10.1061/40743(142)8.

Ukritchon, B. and Keawsawasvong, S. (2016). "Undrained pullout capacity of cylindrical suction caissons by finite element limit analysis." *Computers and Geotechnics*, Vol. 80, pp. 301-311, DOI: 10.1016/j.compgeo.2016.08.019.

Ukritchon, B. and Keawsawasvong, S. (2017). "Unsafe error in conventional shape factor for shallow circular foundations in normally consolidated clays." *Journal of Geotechnical and Geoenvironmental Engineering*, Vol. 143, No. 6, pp. 02817001, DOI: 10.1061/(ASCE)GT.1943-5606.0001670.

Ukritchon, B., Yoang, S., and Keawsawasvong, S. (2017). "Bearing capacity of shallow foundations in clay with linear increase in strength and adhesion factor." *Marine Georesources and Geotechnology*, DOI: 10.1080/1064119X.2017.1326991.